Electromagnetic Generation of Ultrasonic Shear Waves in Potassium †

G. Turner,* R. L. Thomas, and D. Hsu
Department of Physics, Wayne State University, Detroit, Michigan 48202
(Received 16 November 1970)

Measurements have been made of the field dependence of both the electromagnetic generation and the attenuation of ultrasonic shear waves along the [110] direction in potassium in the nonlocal limit. In this limit in the configuration where the Lorentz force is responsible for the generation, the sound amplitude is nonlinear in the magnetic field strength through the region of the Kjeldaas absorption edge. We also observe an electromagnetically generated shear sound wave which is present at zero field and polarized at right angles to the direction of the rf magnetic field axis, and whose efficiency of generation drops nearly to zero at the Kjeldaas edge. The existing free-electron theory has been extended to the anisotropic case, and the experimental results are compared with theoretical predictions for both free-electron and charge-density-wave models of the Fermi surface using an experimental determination of the electron mean free path.

I. INTRODUCTION

A number of recent experiments[1-8] have demonstrated that ultrasonic shear waves can be generated at the surface of a metal by impinging electromagnetic radiation. In the presence of a static longitudinal magnetic field, the sound polarization is found to be parallel to that of the rf magnetic vector when the conductivity takes the value appropriate to the classical (local) limit and arises from the Lorentz force on the eddy currents in the surface. As a result, a characteristic feature of the effect in this limit is that the generated sound amplitude is linear in the strength of the applied magnetic field. Most of the experimental investigations reported in the literature have been carried out in this local limit, for which linearity has been confirmed up to 140 kG.

Generation in the absence of a magnetic field was reported by Abeles[5] for microwave frequencies in thin indium films, and has recently been observed in aluminum and tungsten at MHz frequencies by Wallace *et al.*,[9] who, although they made no quantitative comparison with theory, correctly pointed out that this shear wave is polarized at right angles to the rf magnetic field vector.

The present work, reported briefly elsewhere,[10] was undertaken to investigate the magnetic field dependence of the efficiency of these two polarizations of generation in the more general nonlocal case when the electron mean free path l is large compared to the sound wavelength. Potassium is soft and reactive, and therefore presents a number of problems which would seem to make it a poor candidate for such experiments. Indeed, the difficulty of ensuring that thin samples had sufficiently flat and parallel faces, coupled with the inherently high acoustic attenuation typical of the metal, did prevent *absolute* generation efficiency measurements which have proved possible, at least in the local limit, for other metals. The only reasonably general theory available was that of Quinn,[11] which made use of a free-electron model for the metal. It appeared evident from the failure of the same model, in describing acoustic attenuation in metals with complicated Fermi surfaces, that in order to make quantitative comparisons with this theory, a metal with a simple Fermi surface was desirable. Although the subject of recent controversy, it appears likely that the Fermi surface of potassium is spherical to within 1%,[12] making this metal a good choice for investigation. An added advantage of investigating potassium was that an extension of the theory to include elastic anisotropy, discussed below, indicated that the unusually large difference in shear velocities for sound propagation along the [110] direction could be exploited to ease the interpretation of experimental results. Further, the controversy over a possible distortion of the Fermi surface due to a proposed charge-density-wave (CDW) modification to the ground state added interest to such measurements for potassium. In fact, the experiments reported here are probably not directly relevant to the controversy, for it must be acknowledged that mechanically bonded transducers are likely to strain the crystal and may mask CDW effects. However, electromagnetic generation of a sound wave and the converse effect of electromagnetic generation by a sound wave would make acoustic experiments on strain-free unbonded crystals possible, allowing experiments[13] on the Kjeldaas absorption edge[14] to be repeated under the stringent conditions which have been suggested to be necessary to give a conclusive test of the CDW hypothesis. As only the local limit of the generation for other metals had previously been investigated, the experiments reported here were considered essential preliminaries to such a project.

Combined generation and detection measurements were carried out on an unbonded sample, but the signal-to-noise ratio to date has been too low in the field region below the Kjeldaas edge to make the results unequivocal.

II. THEORY

At present, no theory of electromagnetic sound generation is available which is valid for general boundary conditions, even for the free-electron model. However, the assumption of specular reflection of electrons at the metal surface allows a calculation which is quite like that of standard ultrasonic attenuation theory. Such a treatment has been outlined briefly by Quinn[11] for an elastically isotropic metal. Subsequent extensions by others[6,7,15,16] have considered limiting cases that are inappropriate to the present experiments. In this section, we shall consider specifically the generation of circularly and linearly polarized shear waves in the nonlocal limit, both for the elastically isotropic metal, with its degenerate shear modes, and for propagation along a twofold symmetry axis of an anisotropic metal, a situation for which the degeneracy in the shear wave velocities is removed.

Following the method outlined by Quinn, [11] the metal is considered to occupy the half-space $z>0$, with an electromagnetic plane wave incident from the vacuum $z<0$, and with a static magnetic field B_0 applied in the z direction. The sound wavelengths greatly exceed interatomic spacings, hence the metal is considered as a free-electron gas with an isotropic background of positive ions. The problem is then converted to one in an infinite metal by noting that, for $z>0$, the boundary condition of specular reflection is satisfied if the motion of all electrons in the infinite metal is made even about $z=0$. The space $z<0$ then "absorbs" electrons incident from the right and "supplies" reflected ones. The boundary conditions appropriate for the equivalent infinite medium problem are, therefore, that transverse electric and magnetic fields are even and odd, respectively, in the z coordinate at the boundary. Continuity of tangential field components allows the boundary conditions to be completed by imposing a finite rf magnetic field at $z=0+$, $(H_x(0), H_y(0), 0)$.

For plane waves of the form $e^{i(\omega t-qz)}$, neglecting displacement currents, Maxwell's equations become

$$\frac{dH_y}{dz}=-\frac{4\pi}{c}J_x,\quad \frac{dE_x}{dz}=-\frac{i\omega}{c}H_y,$$

$$\frac{dH_x}{dz}=\frac{4\pi}{c}J_y,\quad \frac{dE_y}{dz}=\frac{i\omega}{c}H_x,$$

where $\vec{J}$ is the macroscopic current density.

The Fourier transforms of these equations can then be taken, using the symmetries and boundary conditions discussed above, to obtain

$$E_x(q)=\frac{-4\pi i\omega}{c^2q^2}J_x(q)+\frac{i\omega}{\pi q^2c}H_y(0),$$

$$E_y(q)=\frac{-4\pi i\omega}{c^2q^2}J_y(q)-\frac{i\omega}{\pi q^2c}H_x(0),$$

which are conveniently combined by writing $E_\pm = E_x \pm iE_y$, etc., appropriate to circular polarized components, giving

$$J_\pm \pm \frac{ic}{4\pi^2}H_\pm(0)=i\beta\sigma_0 E_\pm, \tag{1}$$

where

$$\beta=\frac{c^2q^2}{4\pi\omega\sigma_0}=2\pi^2\left(\frac{\delta}{\lambda}\right)^2,$$

δ is the classical skin depth, and λ is the acoustic wavelength.

The total current $J_\pm$ can be resolved into its electronic (J_e) and ionic (J_I) components. The electronic component can be related to the electric fields by solving Boltzmann's equation, yielding

$$J_\pm(q)=J_I+J_e$$

or

$$J_\pm(q)=ine\omega r_\pm(q)+\sigma_\pm\left(E_\pm(q)-\frac{m}{\tau e}\frac{\partial r_\pm}{\partial t}\right), \tag{2}$$

where $r_\pm$ are the lattice displacements and $\sigma_\pm = \sigma_{xx}\mp i\sigma_{xy}$ are combinations of the magnetoconductivity tensor components.

Equations (1) and (2) combine to give the following relationship between the Fourier transforms of the lattice displacements and electromagnetic fields:

$$E_\pm(q)=\frac{ine\omega}{\sigma_0}\frac{\sigma_\pm-\sigma_0}{\sigma_\pm-i\beta\sigma_0}r_\pm(q)\mp\frac{ic}{4\pi^2}\frac{H_\pm(0)}{\sigma_\pm-i\beta\sigma_0}. \tag{3}$$

A. Isotropic Case

The equations of motion for the ions can be written as

$$M\frac{\partial^2 r_\pm}{\partial t^2}=Ms^2\frac{\partial^2 r_\pm}{\partial z^2}+ZeE_\pm\mp\frac{Ze}{c}iB_0\frac{\partial r_\pm}{\partial t}-\frac{Zm}{ne\tau}\left(J_e+ne\frac{\partial r_\pm}{\partial t}\right), \tag{4}$$

where M is the ionic mass, B_0 is the external magnetic field, $r_\pm$ are the lattice displacements, s is the velocity of sound, and Ze is the ionic charge. The last term in Eq. (4) arises from the τ^{-1} collisions/sec of the electrons having a mean velocity $-J_e/ne$ with the moving ions. The other terms in Eq. (4) represent the short-range elastic forces and the Lorentz force on the ions. Taking the Fourier transform of Eq. (4), with $r_\pm$ even about the boundary, $(\partial r_\pm/\partial z)_{z=0}=0$, and using Eqs. (2) and (3), we have

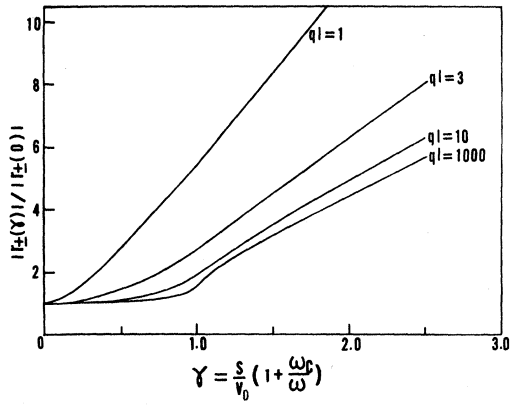

FIG. 1. Generation amplitude for circularly polarized waves in the Kjeldaas approximation for an elastically isotropic metal. In each case, the curves are normalized to the generation in zero field and the difference between the two senses of polarization is too small to display.

$$\left[q^2s^2 - \omega^2\left(1 \pm \frac{\Omega_c}{\omega} + P_\pm\right)\right] r_\pm = \frac{\omega}{\pi i} K_\pm \ , \tag{5}$$

where

$$P_\pm = \frac{Zmi}{M\tau\omega} \frac{(1-i\beta)(1-\sigma_0 R_\pm)}{1-i\beta\sigma_0 R_\pm} \ ,$$

$$K_\pm = \mp \frac{Zec}{M\sigma_0 4\pi\omega} \frac{1-\sigma_0 R_\pm}{1-i\beta\sigma_0 R_\pm} H_\pm(0) \ ,$$

Ω_c is the ion cyclotron frequency, and $R_\pm = 1/\sigma_\pm$. This result is just that of Quinn.[17]

Equation (5) possesses plasmon (or helicon) solutions, but for the present we shall consider only values of the magnetic field B_0 such that these solutions are highly damped; the terms have therefore been grouped to make the acoustic solutions more apparent.

Taking the inverse Fourier transform of Eq. (5), and using the boundary conditions on incoming and outgoing waves at infinity to perform the contour integral, we have

$$r_\pm = (K_\pm/s)\, e^{-i(\omega X_\pm/s)z} \ , \tag{6}$$

where

$$X_\pm = 1 \pm \frac{\Omega_c}{2\omega} + \frac{P_\pm}{2} \ .$$

We have assumed only small changes in the real part of q from its zero-field value and that the imaginary part of q is small. Equation (6) describes damped circularly polarized acoustic waves, which can be generated independently by correspondingly polarized electromagnetic waves. The attenuation and dispersion relations can be obtained from the imaginary and real parts of $X_\pm$, respectively, and are identical to results found in the literature. The generated amplitude described by Eq. (6) is complex in general, and therefore also includes the field dependence of the phase of the displacement relative to the rf driving fields. Equation (6) reduces to a particularly simple and universal form when terms containing the parameter β can be neglected. In this case (the Kjeldaas approximation), Eq. (6) leads to

$$r_\pm(z=0) = \mp \frac{cZe}{4\pi M\sigma_0\omega s}(1-\sigma_0 R_\pm) H_\pm(0). \tag{7}$$

Figures 1 and 2 illustrate the amplitude and phase of the wave leaving the boundary in this approximation, when use is made of the explicit values of $\sigma_\pm$ in terms of ql as given by Kjeldaas[14] for the free-electron case.

The linearly polarized solutions are obtained by noting that $\sigma_-(\gamma) = \sigma_+^*(\gamma)$, where the asterisk denotes the complex conjugate, and $\gamma = (s/v_0)[1+(\omega_c/\omega)]$, where v_0 is the Fermi velocity. Thus, typically for $B_0 > 100$ G, such that $\omega_c \gg \omega$, we have $\sigma_-(B_0) \simeq \sigma_+^*(B_0)$. This leads to a generated wave

$$r_\pm(z=0) \sim (\mp a - ib) H_\pm(0) \ , \tag{8}$$

where a and b are the real and imaginary parts of $(1-\sigma_0 R_\pm)$, respectively. If arbitrarily we choose the incident wave to have its magnetic vector polarized in the x direction, we have

$$r_x(0) \sim b\, H_x(0), \quad r_y(0) \sim a H_x(0), \tag{9}$$

so that the real and imaginary parts of $(1-\sigma_0 R_\pm)$ determine lattice displacements at the surface parallel to the rf electric and magnetic field vectors, respectively. These two components of the ultrasonic shear wave have different physical origins. The component of sound generation parallel to the rf electric vector is largest at the very low fields $\omega_c \sim \omega$, falls to vanishingly small values when $\omega_c \tau > ql$, and results from the same interaction responsible for the high attenuation of a propagating

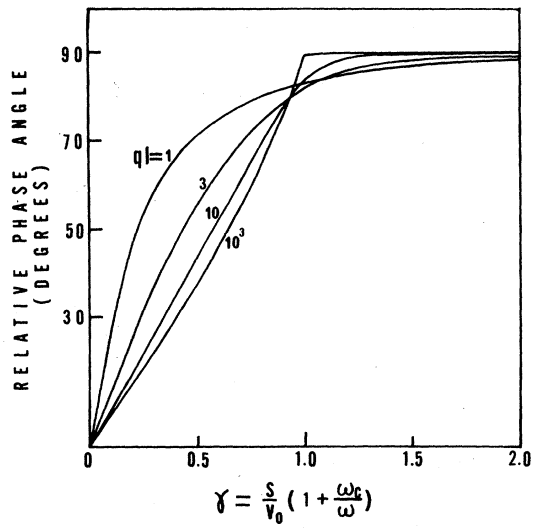

FIG. 2. Phase, relative to the rf driving fields, of circularly polarized shear waves in the Kjeldaas approximation.

shear wave in this field region, i.e., Doppler-shifted cyclotron resonance. The attenuation, given by the imaginary part of $P_\pm$, differs from the form of the generation described by Eq. (6) only through the field-independent factor $(1-i\beta)$, so that in the approximation $\beta \ll 1$ considered here, the two are identical. The theoretical plots of this generation mechanism, shown in Fig. 3, are, therefore, the same as predicted by Kjeldaas for the *attenuation*. In the case of potassium at liquid-helium temperatures, it is the term $(1-i\beta\sigma_0 R_\pm)$ common to attenuation and generation in Eq. (5) which introduces the largest error in the approximation used to obtain Eq. (9); thus, one can see that this similarity between the field dependence of the attenuation and generation is reasonably general.

The classical limiting form of the component of sound having polarization parallel to the rf magnetic vector follows directly from Eq. (9). In the local limit $\omega_c\tau \gg ql$ it is easily shown that $\sigma_0 R_\pm = 1 \mp i\omega_c\tau$, and when the constant terms are retrieved we obtain for the linearly polarized incident wave

$$r_x(0) = -i[H_x(0)/4\pi\rho\omega s]B_0 ,$$

where ρ is the density. The lattice displacement is linear in the static magnetic field, as expected from a physical interpretation in terms of the Lorentz force on the surface eddy currents. At lower magnetic fields corresponding to the non-local conditions, electrons which interact with the surface fields have collisions at distances into the metal comparable to an acoustic wavelength. The effective "smearing" of the Lorentz force leads to less efficient generation by a factor dependent on ql which we have calculated numerically for $\beta \to 0$ and display in Fig. (4) for several values of ql.

The discussion above indicates that the use of

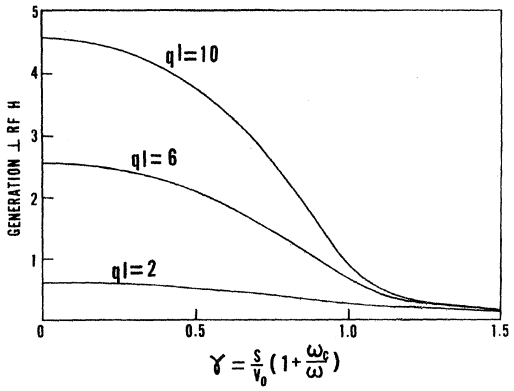

FIG. 3. Field dependence of the amplitudes (calculated in the Kjeldaas approximation) of shear waves generated with polarization perpendicular to the rf magnetic field. These curves also give the field dependence of the attenuation in this approximation.

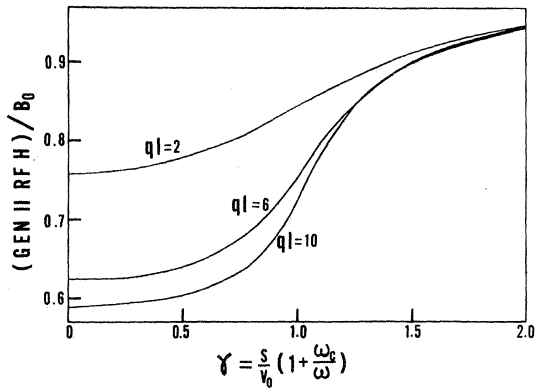

FIG. 4. *Deviation* from linearity in the Kjeldaas approximation for sound generation with polarization parallel to the rf magnetic field. Curves are normalized to the local (high-field) limit.

linearly polarized waves in principle allows the separate measurement of the two physical processes involved in the generation described by the theory. However, there is a complication in that linearly polarized waves are *not* pure modes for the lattice in an applied magnetic field, and, therefore, after generation they do not propagate unchanged. A linearly polarized wave is resolved by the lattice into two circular components which propagate as described by Eq. (6) with different velocities and attenuations and which, when recombined at a receiving transducer, will lead to a field-dependent rotation of the plane of polarization[18] and introduce considerable complication into the interpretation of experimental results.

B. Anisotropic Case

For the elastically anisotropic metal, Eqs. (1)–(3) are retained and only Eq. (4) is modified. We take the x and y axes to lie along the directions of pure shear polarizations so that when only the short-range ionic forces are included we have

$$\frac{\partial^2 r_x}{\partial t^2} = s_x^2 \frac{\partial^2 r_x}{\partial z^2}$$

and

$$\frac{\partial^2 r_y}{\partial t^2} = s_y^2 \frac{\partial^2 r_y}{\partial z^2} .$$

The Fourier transform for the complete equation of motion then becomes

$$-M\omega^2 r_\pm = -\tfrac{1}{2}M[q^2 s_x^2(r_+ + r_-) \pm q^2 s_y^2(r_+ - r_-)]$$
$$+ZeE_\pm \mp \frac{Ze}{c} iB_0 \frac{\partial r_\pm}{\partial t} - \frac{Zm}{ne\tau}\left(J_e + ne\frac{\partial r_\pm}{\partial t}\right) . \quad (10)$$

Combining Eqs. (2), (3), and (10) leads to a result corresponding to Eq. (5):

$$\tfrac{1}{2}q^2(s_x^2 \pm s_y^2)r_+ + \tfrac{1}{2}q^2(s_x^2 \mp s_y^2)r_- - \omega^2\left(1 \pm \frac{\Omega_c}{\omega} + P_\pm\right)r_\pm$$

$$=\frac{\omega}{\pi i} K_{\pm} \ . \tag{11}$$

We have solved these coupled equations assuming small changes in the real part of q and assuming that the imaginary part is small. After taking the inverse Fourier transform, we find that the generation of two modes is given by

$$\begin{aligned} r_P(z) &= (K_P/s_x)e^{-i\omega z Y/s_x}, \\ r_Q(z) &= (K_Q/s_y)e^{-i\omega z Y/s_y}, \end{aligned} \tag{12}$$

where

$$\begin{aligned} r_P &= (1-\tfrac{1}{2}\gamma_P)r_+ + (1+\tfrac{1}{2}\gamma_P)r_- , \\ r_Q &= (1+\tfrac{1}{2}\gamma_Q)r_+ - (1-\tfrac{1}{2}\gamma_Q)r_- , \\ K_P &= (1-\tfrac{1}{2}\gamma_P)K_+ + (1+\tfrac{1}{2}\gamma_P)K_- , \\ K_Q &= (1+\tfrac{1}{2}\gamma_Q)K_+ - (1-\tfrac{1}{2}\gamma_Q)K_- , \\ \gamma_P &= \frac{s_x^2}{s_x^2 - s_y^2}\left(P_+ - P_- + 2\,\frac{\Omega_c}{\omega}\right), \\ \gamma_Q &= \frac{s_y^2}{s_x^2 - s_y^2}\left(P_+ - P_- + 2\,\frac{\Omega_c}{\omega}\right), \\ Y &= 1 + \tfrac{1}{4}(P_+ + P_-), \end{aligned}$$

and $K_{\pm}$ and $P_{\pm}$ are defined in Eq. (5). These equations describe the generation of two shear modes which, in general, are elliptically polarized, propagate with different velocities and attenuations, and could be excited independently by suitably polarized electromagnetic waves. For propagation along a $\langle 110\rangle$ direction in potassium, the large difference in shear velocities justifies the assumption that γ_P and γ_Q are small, so that the modes are almost linearly polarized. Thus, solution of Eq. (12) to obtain the components of the displacement yields

$$r_x = \left(\frac{K_P}{2s_x}\right) e^{-i\omega z Y/s_x} + \frac{\gamma_P}{4}\left(\frac{K_Q}{s_y}\right) e^{-i\omega z Y/s_y}, \tag{13}$$

and a similar equation for r_y. The two components of r_x propagate with different velocities and therefore may be measured separately in a pulsed experiment. In the Kjeldaas[14] approximation, taking a and b to be the real and imaginary parts of $(1-\sigma_0 R_{\pm})$, the driving term of the larger component of r_x (which propagates with velocity close to s_x) is given by

$$K_P \sim (a\gamma_P - 2ib)H_x(0) - (b\gamma_P + 2ia)H_y(0) \ . \tag{14}$$

We see that the real and imaginary parts of $(1-\sigma_0 R_{\pm})$ couple the wave amplitude to the components of the rf magnetic vector perpendicular and parallel to the sound polarization, respectively, which is just the result which might be intuited from the discussion of the isotropic metal. For a sufficiently anisotropic metal with almost linearly polarized shear modes, there are no complications arising from propagation except for simple attenuation, and the use of a linearly polarized electromagnetic wave, as in the experiments reported here, allows resolution of the two physical processes involved.

III. EXPERIMENTAL

A. Samples

Measurements were made on a single crystal of potassium in the shape of a disc about 3 cm in diam and 5 mm thick with its plane and parallel faces cut to lie in the (110) crystallographic planes. Transmission x-ray photographs supplied with the specimen indicated that the alignment was within 1°. Shear sound velocities of 1.74×10^5 and 0.648×10^5 cm/sec were measured at 4.2 °K and 10 MHz, although the slow shear velocity exhibited a noticeable field dependence and increased to 0.676×10^5 cm/sec on changing the field from 0 to 60 kG.

The sample surface used for generation measurements was freshly etched before each run and a measured bulk relaxation time should therefore also be reasonably representative of the value within the skin depth, the only important region for electromagnetic generation. The electron mean free path in the sample was estimated experimentally by measuring the longitudinal wave ultrasonic attenuation at 4.2 °K as a function of the transverse magnetic field strength at the odd harmonics of an x-cut quartz transducer from 10 to 110 MHz. According to the free-electron model,[19] the change in longitudinal wave attenuation in a strong magnetic field may be written as

$$\lim_{B_0\to\infty}[\alpha(B_0) - \alpha(0)]$$

$$= \frac{2\pi n m v_0 f}{\rho s^2}\left(\frac{ql}{15} + \frac{1}{ql} - \frac{ql\tan^{-1}ql}{3(ql-\tan^{-1}ql)}\right) \ , \tag{15}$$

where n is the number of free electrons per unit volume, m is the electron mass, f is the ultrasonic frequency, and v_0 is the Fermi velocity. Since theory predicts that the high-field limiting attenuation is approached as B_0^{-2}, $\lim\alpha(B_0)$ as $B_0\to\infty$ was determined by extrapolation from the highest (~14 kG) field measurements. The measured attenuation was compared to Eq. (15) for each frequency to obtain an estimate of the relaxation time $\tau = l/v_0$. The best estimate of τ from these measurements is $\tau = 0.7\times10^{-10}$ sec, which proves to be consistent with the measurements of the shear wave attenuation in a longitudinal field, discussed below.

B. Technique

Measurements were made at 4.2 °K using a conventional ultrasonic pulse-echo apparatus.[20] In order to improve the signal-to-noise ratio, however, low-noise tuned preamplifiers were em-

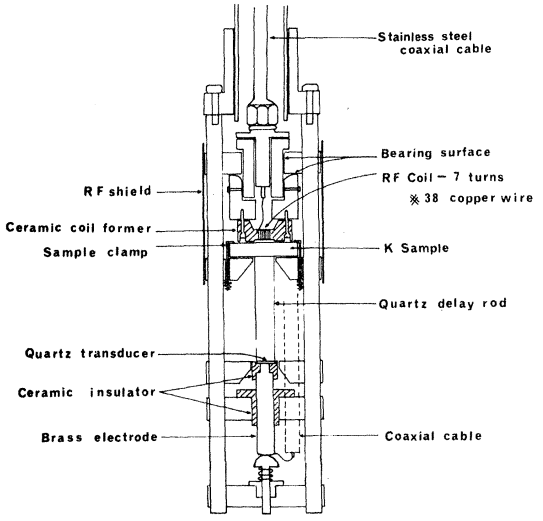

FIG. 5. Schematic drawing of the sample holder.

ployed. The other modification to the apparatus was to replace one of the transducers by a small rf coil which was placed near the potassium sample with its axis rotatable in a plane parallel to the sample face. The sample was held by very lightly sprung clamps in a holder shown schematically in Fig. (5).

Most of the measurements to be reported below were made transmitting on the coil and receiving on an *ac*-cut quartz transducer, which was separated from the opposite face by a 3-cm-long x-cut quartz delay rod. Some measurements were made with transmitter and receiver reversed, and attenuation measurements were made by replacing the coil with a second transducer.

By rotating the coil, it was possible to excite preferentially either the fast or slow shear modes in the potassium sample, although for magnetic field strengths below the Kjeldaas[14] absorption edge, it was possible to observe generation with the rf magnetic field either perpendicular or parallel to the respective shear polarization directions. The transmitted echo height was measured at the transducer as a function of frequency and magnetic field by a box-car integration circuit,[21] and displayed on a strip-chart recorder. The peak echo voltage was calibrated by coupling to the preamplifier a suitably synchronized and time-delayed pulse from a signal generator and calibrated attenuator. The frequency was determined by observing a zero-beat signal on an oscilloscope between the signal generator (operated cw) and the displayed echo train. The signal generator in turn was monitored with a digital frequency meter.

The magnetic field was supplied by a 60-kG superconducting solenoid and measured using a magnetoresistance probe which was calibrated by proton NMR measurements. For magnetic fields above 5 kG, the absolute field strength was known to better than 100 G.

IV. RESULTS

A. Attenuation

Suitable corrections for the attenuation during propagation through the sample were required to obtain the field dependence of the generated amplitude. Ideally, data for this purpose might have been obtained in the same run as the generation data by using the quartz transducer to make single-ended attenuation measurements. In practice, the large reflections at the interface between sample and delay rod made such measurements unreliable, and a separate set of experiments in which the rf coil was replaced by a second transducer were used to provide attenuation data. Typical results are displayed in Fig. 6, where they are compared with the theoretical attenuation calculated from a free-electron Fermi surface and also for the "lemon"-shaped distortion predicted for a CDW model of the ground state. In performing numerical calculations based on Eq. (5), the experimentally determined relaxation time was used. It should be noted, therefore, that no adjustable parameters were necessary in comparing theory and experiment.

We repeat that care must be exercised in using these attenuation results to draw conclusions about the existence of a CDW ground state. The present experiments are open to the same objections as earlier acoustic work, in that the sample is almost certainly strained by the bonding of a transducer at one face. These results primarily give confidence in using the free-electron model to correct

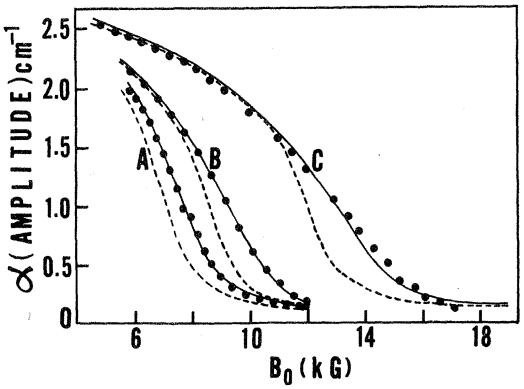

FIG. 6. Comparison of experimental attenuation along the [110] axis of potassium with computer calculations from Eq. (12) using free-electron (FE) and charge-density-wave (CDW) models of the Fermi surface: (a) slow shear mode at 17.6 MHz; (b) fast shear mode at 60.3 MHz; and (c) slow shear mode at 30.5 MHz.

the generation data taken under closely similar experimental conditions on the same sample and generally at only slightly different frequencies. All the data for generation presented below were obtained by making such theoretical attenuation corrections.

B. Generation Amplitudes

The generation of both fast and slow shear modes was studied, but for the relatively thin sample used, data for the fast shear mode were considered to be more reliable. The first transmitted pulse of the fast mode was well separated in time from the other echoes, whereas the first slow shear pulse was close to the first echo of the fast shear mode (three passes in the sample) and generally much smaller, because the acoustic Kjeldaas edge for the slower shear mode occurs for a much higher magnetic field. The quantitative results presented here will be exclusively for the fast shear mode.

The field dependence was measured for the two geometries in which the rf magnetic field is either aligned parallel or perpendicular to the shear polarization direction. Absolute measurements for generation require absolute attenuation corrections. The attenuation was large in the nonlocal limit, however, and often only a single echo was detectable. Furthermore, since diffraction effects are not negligible in these relatively thin soft samples, absolute generation measurements were not feasible in the present experiment. However, a technique was devised in which the relative efficiencies of the two geometries were compared as a function of static magnetic field by finding the angular position of the coil corresponding to the minimum signal generation.

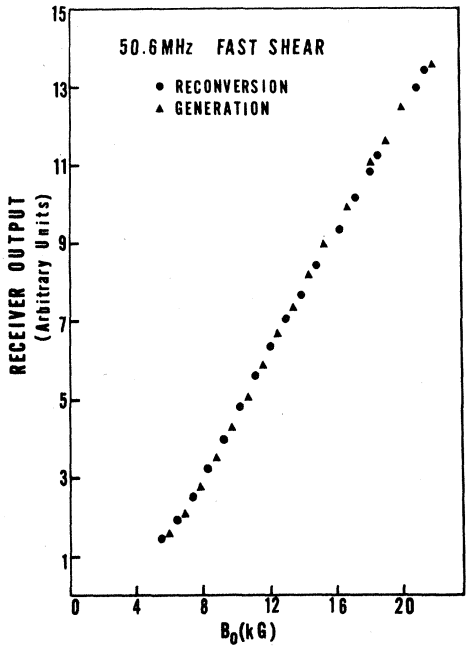

FIG. 7. Comparison of the received signal amplitude when (a) the transmitter was connected to the coil (generation) and (b) when the transmitter was connected to the transducer and the coil to the receiver (inverse effect). Note that the amplifier is nonlinear and that the raw signal also includes attenuation losses, both of which must be allowed for in obtaining the true conversion efficiency.

1. *Generation with* rf *Magnetic Field Parallel to Sound Polarization*

This is the geometry required for efficient generation in the local limit and for which no generation is expected in zero field. The coil position could be set either as the angle for maximum signal at large fields or zero signal at low fields with no significant difference. Such settings were within $\pm 5^\circ$ of the corresponding conditions as deduced from the known crystal orientation. Measurements were made at frequencies close to 10, 30, and 50 MHz by exciting the rf coil by the transmitter and receiving on a transducer and delay rod. No significant difference in field dependence was obtained by switching the transmitter and receiver (Fig. 7).

The dominant feature of the results is a large, almost linear, field dependence of the generated amplitude (Figs. 8 and 9). The comparison with theory has therefore been made more sensitive by comparing experimental and theoretical *deviations* from linear behavior (Fig. 10). The large change in received signal amplitude over significant field intervals taxed the dynamic range of the instrumentation, making it difficult to maintain high relative accuracy. Resultant possible systematic errors were such that the deviations between theory and experiment are estimated to lie within the experimental uncertainty. An interesting exception was found in one of the coil-transducer runs at 50 MHz for which the generation behavior differed markedly from the theory in being almost exactly linear over the full field region.[10] However, on inspection of the sample after the run, it was found that the coil had made partial contact with the surface of the sample during rotation, with resulting surface damage to the sample. Thus, although attenuation measurements taken in the same experimental run indicated that the bulk electron relaxation time was unchanged, the relaxation time within the rf skin depth presumably had been lowered substantially for this run. After the damaged layer was removed by etching, the measurement was repeated and yielded results similar to those in the lower part of Fig. 1 in Ref. 10.

2. *Generation with* rf *Magnetic Field Perpendicular to Sound Polarization Direction*

This geometry proved to be a much more difficult

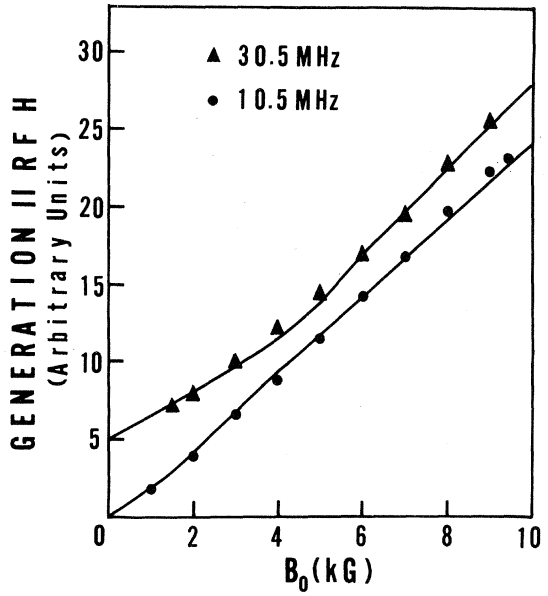

FIG. 8. Field dependence of the generation amplitude with sound polarization parallel to the rf magnetic field: fast shear mode at 10.5 and 30.5 MHz. Solid curves are computer calculations from Eq. (12) for a spherical Fermi surface and experimentally determined relaxation time $\tau = 0.7 \times 10^{-10}$ sec. Note that for clarity the 30.5-MHz curve is displaced from the origin by five units along the ordinate.

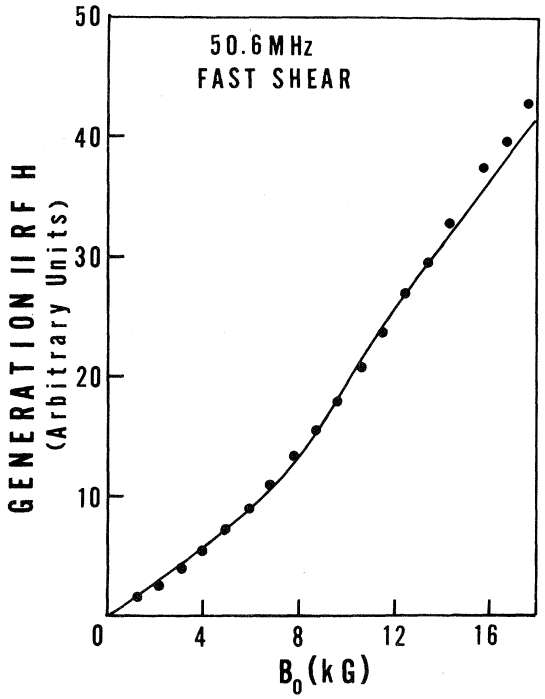

FIG. 9. Same as Fig. 8: fast shear mode at 50.6 MHz.

one in which to obtain consistent results. This resulted in part from the small-signal levels, for the generation was greatest at zero field, where the attenuation was high, and low at high fields, where the attenuation is small, resulting in a received signal which was never large.

Rotation of the coil at zero field showed the expected maximum with the coil axis perpendicular (to within ±5°) to the sound shear polarization direction. With the coil set at the position for maximum zero-field signal, the field dependence of the generated signal was then measured. The generation from any small component of the rf magnetic field parallel to the shear axis is very large at higher fields, where the component investigated here should give a vanishingly small contribution. Using the measurements discussed above for the previous geometry, a correction was then made allowing for the presence of this component at lower fields, yielding results shown in Figs. 11 and 12. One disconcerting feature of this procedure was that the measured amplitude had a stronger field dependence in the high-field region than could be explained reasonably by the assumption of a component of the unwanted polarization; it was, in fact, stronger than that measured directly for the latter geometry. This shows up in Figs. 11 and 12 as a rise in the corrected generation amplitude at high fields. At the time these measurements were taken, it was considered that the disagreement with theory over this feature arose through the use of the Kjeldaas approximation then in use. However, the discrepancy is not removed even in the fuller theory used here and is not understood. It should perhaps be emphasized that the component signals involved in this discrepancy are much smaller than

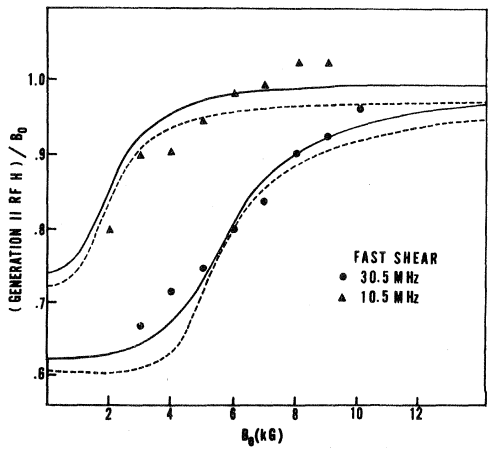

FIG. 10. Explicit display of the *deviation* from linearity, i.e., the change of slope of the curves in Fig. 8. Solid curves are calculated from Eq. (12) for $\tau = 0.7 \times 10^{-10}$ sec and a spherical Fermi surface; dashed curves show results of calculations using the "lemon"-shaped Fermi surface appropriate to a CDW ground state.

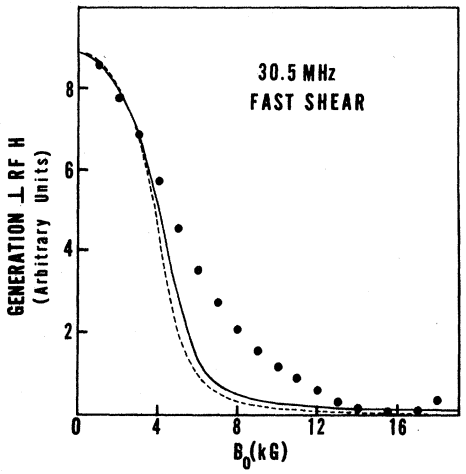

FIG. 11. Generation amplitude for the fast shear mode polarized perpendicular to the rf magnetic field at 30.5 MHz, after subtracting a signal proportional to the generation parallel to the rf magnetic field. Solid and dashed curves correspond to FE and CDW theories, respectively.

those found for the direct geometry (coil axis parallel to the sound polarization), so that quite a small perturbation of the latter might account for the observed results.

3. *Relative Measurements*

Simple comparison of the generation efficiencies for the two geometries discussed above is made difficult by the sensitivity of generation to the exact coil position and, in particular, to its distance from the sample. Therefore, measurements of the relative generated amplitudes for the two geometries were made directly by finding the angular position of the coil which gave minimum[22] signal as the magnetic field B_0 was varied. For zero field, this position was such that the rf magnetic field was parallel to the shear axis. As the magnetic field was raised above the Kjeldaas edge, the angular position of the minimum changed by 90°. Experimental results are compared with the theoretical predictions in Figs. 13–15.

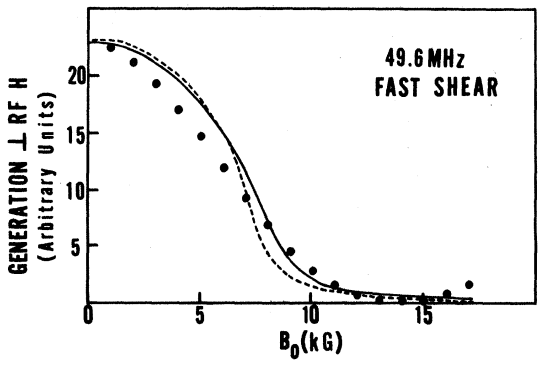

FIG. 12. Same as Fig. 11 at 49.6 MHz.

V. DISCUSSION

The agreement between the results presented in Sec. IV and the theory of Sec. II is substantial. For the generation of shear waves polarized parallel to the rf magnetic field, our measurements certainly show the departures from linearity in B_0 predicted by the theory for the nonlocal limit, and the importance of the mean free path within the skin depth has also been clearly demonstrated. In the orthogonal geometry, where generation is only predicted for nonlocal conditions, the experimental difficulties were most severe and quantitative agreement with theory was poorest. In particular, the small but consistent disagreement for the generation in this geometry at fields just above the Kjeldaas edge, where the experiments indicated an unexpected increase in generation efficiency, remains unexplained. However, instrumental problems cannot be ruled out completely as rather large corrections were necessary to allow for what was presumably the imperfect experimental geometry. The overall agreement with theory for this geometry, therefore, is considered to be reasonable.

Potassium was chosen for this work with the objective of satisfying the basic free-electron assumptions made in the theory, so that some degree of success was to be anticipated. However, the apparent success of the theoretical assumption of specular reflection of electrons at the metal surface is somewhat surprising. Although Penz and Kushida[23] have reported helicon experiments in potassium which indicate specular reflection in

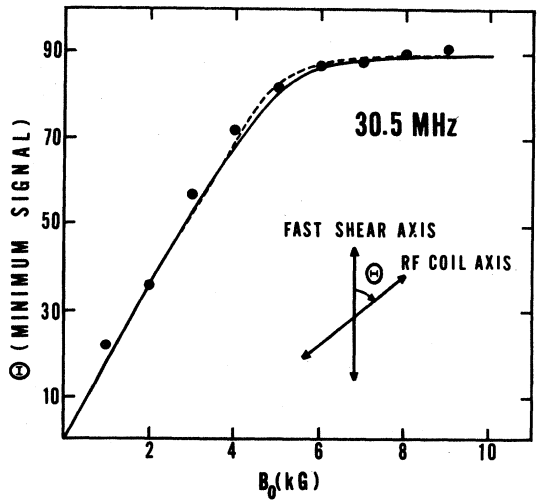

FIG. 13. Experimental points showing the angle for minimum signal as a function of magnetic field B_0 at 30.5 MHz. Solid and dashed curves are calculated using FE and CDW models of the Fermi surface, respectively.

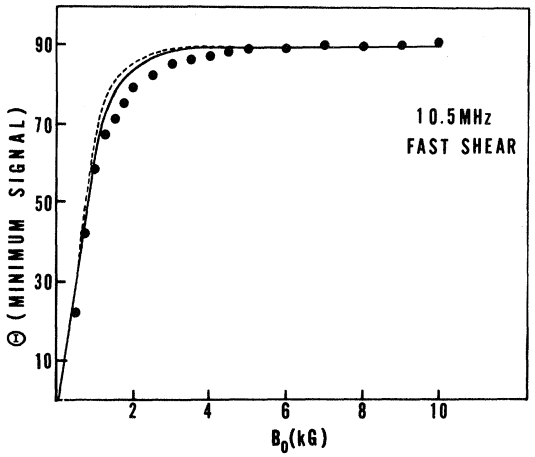

FIG. 14. Same as Fig. 13 at 10.5 MHz.

samples prepared under oil between glass plates, it would seem that for the lapped and etched samples used here, diffuse scattering would be a more appropriate assumption. In contrast to the situation found by Alig[15] at microwave frequencies, the nature of the surface scattering apparently is not crucial in the present frequency range.

An interesting feature of the results in Sec. IV is that the roles of transducer and coil as detector and receiver could be reversed without detectable change in signal. Evidently, the inverse process, in which an electromagnetic wave is generated by a sound wave, has the same field dependence and much the same efficiency as we have found for sound generation by an electromagnetic wave. Such a result is, in fact, indicated by the theory of Sec. II. Thus, consider a shear wave incident from the right and subsequently reflected by a metal vacuum interface. The continuity of tangential field components, and the absence of any incoming electromagnetic wave, allows us to write, for the fields just inside or outside the metal,

$$E_{\pm} = \pm iH_{\pm} .$$

Equation (3) in Sec. II then suggests[24] that at fields away from the helicon-phonon crossover field

$$H_{\pm}(0) = \pm \frac{ne\omega}{\sigma_0} \frac{1 - \sigma_0 R_{\pm}}{1 - i\beta\sigma_0 R_{\pm}} r_{\pm}(0) ,$$

where $r_{\pm}(0)$ will be just twice the amplitude of the incident acoustic wave, assumed here to be perfectly reflected. This result displays the same field dependence and relationships between the relative polarizations as found for the generation of sound waves by a reflected electromagnetic wave, and in the local limit leads to exactly the same generation efficiency, defined as the fraction of incident power converted.

It would be of considerable interest to extend the present work to other metals, where the theory will almost certainly require modification, and also to higher fields where strong interaction between helicons and phonons takes place. Attempts were made during the course of this work to investigate the helicon-phonon interaction, but the experimental problems presented by the large velocity changes and pulse dispersion, coupled with the dramatic changes in polarization of the propagating modes, made interpretation of our results difficult. One of the more interesting complications we found was the simultaneous generation of both soundlike and heliconlike modes in the field region above both Kjeldaas edges. Investigation in this field region would probably be somewhat easier using circularly polarized shear waves along an axis of higher symmetry, although frequencies and fields higher than those used in the present work would be required.

Finally, we would like to make a general observation suggested by the physical interpretations of the generation mechanisms discussed in this paper. The obvious generalization to be made is that where there is structure in the field dependence of the attenuation, there also should be corresponding structure in the generation efficiency, brought about by the same electron-phonon interaction. Recent experiments in this laboratory[25] have emphasized this for the case of quantum oscillations, and have also shown that the effects of interest may indeed be more pronounced in the generation process.

ACKNOWLEDGMENTS

The authors wish to thank Dr. H. V. Bohm, Dr. E. R. Dobbs, and Dr. L. D. Favro for helpful discussions.

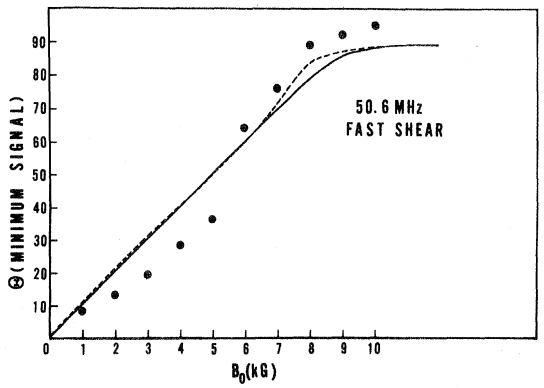

FIG. 15. Same as Fig. 13 at 50.6 MHz. The apparent kink in the experimental points was reproducible for this sample.

†Research sponsored by the U. S. Air Force Office of Scientific Research, Office of Aerospace Research under AFOSR Grant No. 68-1494A.

*Present address: University of East Anglia, Norwich, England.

[1]P. K. Larsen and K. Saermark, Phys. Letters 24A, 374 (1967); 24A, 668 (1967); 26A, 296 (1968).

[2]J. R. Houck, H. V. Bohm, B. W. Maxfield, and J. W. Wilkins, Phys. Rev. Letters 19, 224 (1967).

[3]A. G. Betjemann, H. V. Bohm, D. J. Meredith, and E. R. Dobbs, Phys. Letters 25A, 753 (1967).

[4]R. L. Thomas, G. Turner, and H. V. Bohm, Phys. Rev. Letters 20, 207 (1968).

[5]B. Abeles, Phys. Rev. Letters 19, 1181 (1967).

[6]D. J. Meredith, R. J. Watts-Tobin, and E. R. Dobbs, J. Acoust. Soc. Am. 45, 1393 (1969).

[7]M. R. Gaerttner, W. D. Wallace, and B. W. Maxfield, Phys. Rev. 184, 702 (1969).

[8]V. F. Gantmakher and V. T. Dolgopolov, Zh. Eksperim. i Teor. Fiz. 57, 132 (1969) [Sov. Phys. JETP 30, 78 (1970)].

[9]W. D. Wallace, M. R. Gaerttner, and B. W. Maxfield, Bull. Am. Phys. Soc. 14, 64 (1969).

[10]R. L. Thomas, G. Turner, and D. Hsu, Phys. Letters 30A, 316 (1969).

[11]J. J. Quinn, Phys. Letters 25A, 522 (1967).

[12]For a recent bibliography of this subject, see, for example, R. L. Thomas and G. Turner, Phys. Rev. 176, 768 (1968).

[13]R. L. Thomas and R. V. Bohm, Phys. Rev. Letters 16, 587 (1966).

[14]T. Kjeldaas, Phys. Rev. 113, 1473 (1959).

[15]R. Casànova Alig, Phys. Rev. 178, 1050 (1969).

[16]P. D. Southgate, J. Appl. Phys. 40, 22 (1969).

[17]Equation (5) differs only in a phase factor $\pm i$ which is absent in the equivalent result of Quinn (Ref. 11).

[18]The difference in attenuation leads to the resultant also being slightly elliptically polarized.

[19]A. B. Pippard, Proc. Roy. Soc. (London) A257, 165 (1960).

[20]N. Tepley, Proc. IEEE 53, 1586 (1965).

[21]G. H. Kamm and H. V. Bohm, Rev. Sci. Instr. 33, 957 (1962).

[22]The minimum rather than maximum was investigated simply to allow full use of instrumental sensitivity.

[23]P. A. Penz and T. Kushida, Phys. Rev. 176, 804 (1968).

[24]In fact, the implied boundary conditions required in the infinite medium approximation prevent direct application of the theory of Sec. II. We take the view that the complications involved here are unlikely to be important physically. Also, note that this result is the same as Eq. (5) in R. C. Alig, J. J. Quinn, and S. Rodriguez, Phys. Rev. 148, 632 (1966).

[25]E. R. Dobbs, R. L. Thomas, and D. Hsu, Phys. Letters 30A, 338 (1969); E. R. Dobbs, J. Phys. Chem. Solids 31, 1657 (1970).

PHYSICAL REVIEW B VOLUME 3, NUMBER 10 15 MAY 1971

de Haas-van Alphen Effect in Mercury†

R. G. Poulsen,* J. S. Moss,‡ and W. R. Datars§

Department of Physics, McMaster University, Hamilton, Ontario

(Received 2 October 1970)

We report the results of a detailed investigation of the de Haas–van Alphen effect in single-crystal mercury. The data were taken for the three major crystallographic planes in magnetic fields extending up to 116 kG and at a temperature of 1.2 °K. The frequencies have been assigned to orbits on the second-band electron-lens surface and on the first-band hole surface. Several new extremal orbits on the first-band surface are reported. The results are in general accord with the Fermi surface deduced from other experiments and from band-structure calculations.

I. INTRODUCTION

There have been several recent studies of the Fermi surface of crystalline mercury. However, there is a need to complete de Haas–van Alphen (dHvA) frequency measurements to a uniform accuracy. This work reports the results of an extensive dHvA experiment to provide more accurate and complete dHvA frequency measurements and to extend the understanding of the Fermi surface of rhombohedral mercury.

Previous dHvA experiments in mercury were carried out by Verkin, Lazarev, and Rudenko,[1] Shoenberg,[2] and Brandt and Rayne.[3] The work of Brandt and Rayne, which was the most extensive of the three, gave dHvA frequencies of several extremal orbits in principal crystallographic planes and the general topology of the Fermi surface of mercury. Other reported work on the Fermi surface of mercury includes cyclotron resonance experiments by Dixon and Datars,[4] magnetoresistance experiments by Datars and Dixon[5] and Dishman and Rayne,[6] and magnetoacoustic experiments by Bogle *et al.*[7] These experimental results are in essential agreement with the Fermi-surface topologies determined from the relativistic-augmented-plane-wave (RAPW) model of Keeton and Loucks,[8] the empirical MAGV model of Dishman and Rayne,[6]